EasyChair Preprint

№ 14662

Edge Enhancement and Dual UNet Fusion Based GAN for Structure Preserving Stain Normalization

Yicheng Zhao, Jiacheng Lu, Bo Li, Hui Ding and Guoping Huo

September 3, 2024

Edge Enhancement And Dual UNet Fusion Based GAN For Structure Preserving Stain Normalization

Yicheng Zhao[1 [0009−0007−5848−1686]], Jiacheng Lu[1 [0009−0002−7920−3814]], Bo Li[1], Hui Ding[1 [0000−0002−1920−7613] (✉)], and Guoping Huo[2 [0009−0006−4504−8149] (✉)]

[1] College of Information Engineering, Capital Normal University, Beijing, China
dhui@cnu.edu.cn
[2] School of Artificial Intelligence, China University of Mining and Technology-Beijing, China
kuoping@cumtb.edu.cn

Abstract. Histopathology is the diagnosis and study of tissue diseases, and staining is a crucial part of its analysis. However, differences in laboratory protocols and scanning devices can often result in significant variations in the appearance of images, imposing obstacles to the diagnosis process. To address this issue, we propose a method called EG-DUNet, which is a GAN-based dual UNet network combined with edge enhancement information. The EG-DUNet network is able to obtain multi-scale feature fusion, which helps capture the shape and structure of cells in tissue sample images. To optimize color consistency, a style loss constraint is incorporated into the proposed network. Compared with current mainstream methods, our experimental results show that the EG-DUNet achieves more competitive performance on the MITOS-ATYPIS-14 contest dataset.

Keywords: Histology Images · Staining Normalization · UNet · Style Loss · Deep Learning.

1 Introduction

Digitized histopathology section images provide a rich source of data for computer-aided diagnosis (CAD) systems.CAD systems empower physicians in pathology diagnosis through automation and intelligence, driving the field of pathology in a more modern and intelligent direction [1–3]. Staining is a crucial step in the preparation process of obtaining Whole Slide Images (WSI) of tissues, as illustrated in Fig. 1, where different physiological tissues are stained with distinct colors for differentiation. During the biochemical staining process, steps such as staining batch, slice thickness, and staining method lead to variations in the physical color of the WSI, while variations in the color of the WSI are also affected by factors such as focusing, imaging resolution, and other imaging digital

parameters [4, 5]. This results in batches of these slides collected from different groups or laboratories showing different staining styles [6].

However, due to the limited generalization ability of existing CAD systems when handling such data, staining deviations significantly decrease the accuracy of these systems [7]. Staining normalization technique can effectively solve the problem of color variation in digital pathology and histopathology section images in CAD systems [8]. Traditional staining normalization methods adjust

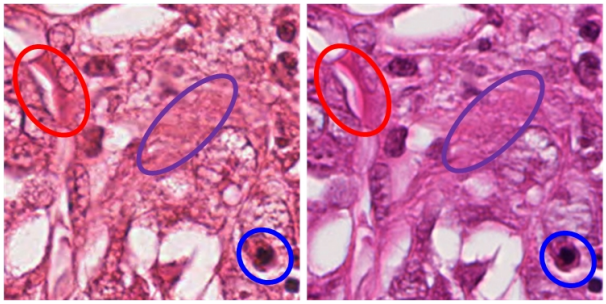

Fig. 1. Nuclei, cytoplasm and collagen fibers staining

color space, luminance distribution, and color correction to make digital pathology section images comparable under various conditions. Reinhard et al [9] proposed a method matching the mean and standard deviation of each channel in the Lab color space. However, this may not completely preserve the background brightness, potentially reducing the source image contrast. Aswathy et al. [10] introduced a two-stage normalization, combining light source and staining normalization to address color fidelity issues. Stain Color Adaptive Normalization (SCAN) [11] enhances tissue-background contrast without altering color and preserves local structure. Conventional color normalization relies on domain experts for reference templates, while deep neural networks, especially generative models, offer a novel approach. Macenko et al. [12] use supervised pixel-level color separation, requiring prior information in the training set. Unsupervised methods like global color normalization Vahadane [13] and structure-preserving color normalization (SPCN) don't guarantee full color information. Deep learning, e.g., CycleGAN [14], addresses these challenges, but CycleGAN masks stained tissue features, limiting model generalization. GANs offer a distinct strategy, with MultiPathGAN [15] proposing a structure-preserving color normalization method based on unsupervised multidomain adversarial networks, using a generator and discriminator for adversarial training to achieve image coloring normalization.

In this work, we design a generative adversarial network based dual Unet network (EG-DUNet) to improve cellular morphology in tissue samples by incorporating edge features. Our method also utilizes a style loss to preserve fine anatomical structures and minimize the perceptual distance between real and generated images. The main contributions are:

- The classic Laplace edge detection operator is used to obtain edge images. Based on H&E (Hematoxylin and Eosin) staining principles, we analyzed the different edge characteristics in the R, G, and B channels to construct an enhanced edge map. Then, the original image fuses with the edge map during encoding.
- A dual UNet architecture fused the original and edge images. One UNet branch downsampled the original image while the other processed the edge image, thereby fusing semantic and edge features.
- We devised a loss function incorporating style loss and an edge feature extraction module to address structural, fidelity and stylistic concerns in medical image normalization.

2 RELATED WORK

2.1 Models Employed in Medical Imaging

MultiPathGAN addresses staining differences in tissue section images arising from factors like diverse laboratories, staining protocols, and scanning devices. Through adversarial training with a generator and discriminator network, MultiPathGAN normalizes image staining by learning mapping relationships across multiple domains. It incorporates an information flow branch and a feature extraction network to optimize perceptual loss and preserve image structural characteristics. While existing models focus on transforming across multiple domains, the staining performance within a single domain is not optimal.

UNet stands as a prominent model extensively applied in the domain of medical imaging. Its distinctive feature, characterized by multi-level down-sampling convolution, aligns well with the high-resolution demands inherent in medical images. The model's heightened convolutional depth, coupled with skip-connection layers, facilitates superior preservation of intricate details within medical images. Employed as a generator, UNet contributes to elevated image quality, thereby facilitating precise pathological assessments by medical practitioners. Furthermore, UNet exhibits a reduced parameter count, leading to expedited training and runtime processes.

2.2 Loss function in staining normalization

The L1 loss $Loss_{L1}$ in pathology slice image normalization helps the generator to produce an output that more closely resembles the target image, ensuring that the generated image is consistent with the real image in terms of detail, structure, and color, and providing a more reliable data base for subsequent pathology analysis. For the generated image $fake\_B$ and the target image $real\_B$, their pixel values are $P_{fake\_B_i}$ and $P_{real\_B_i}$, respectively. L1 loss is calculated as the absolute difference between them:

$$Loss_{L1} = L1_{penalty} \cdot \frac{1}{N} \sum_{i=1}^{N} \left| P_{fake\_B_i} - P_{real\_B_i} \right| \tag{1}$$

Where N is the number of pixels in the image and L1 loss is the pixel level difference between the generated image and the target image. It helps to generate an output closer to the target image. The L1 loss focuses only on the differences between pixel values without taking into account the high-level semantic information and texture details of the image. As a result, it cannot effectively preserve the subtle features and stylistic characteristics of the target image, making it difficult for the generated image to be stylistically identical to the target image in some cases.

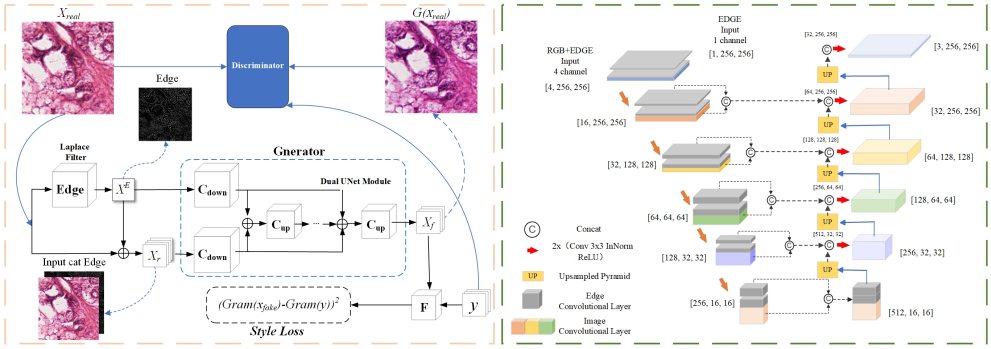

(a) The structure of the EG-DUNet (b) Generator structural of the Dual UNet

Fig. 2. EG-DUNet network and the specific Dual UNet module

3 METHOD

3.1 Architecture of EG-DUNet

In this paper, to address issues such as inconsistent staining and structural inconsistencies in medical pathology images, we design an EG-DUNet for normalization of digital histopathology slides. As shown in Fig. 2, we incorporated a customized Laplacian edge extraction module, coupled with a dual UNet architecture, and a stylistic loss function tailored for stain normalization.

X_{real} is the original input, which, after using the Edge operator, outputs a single-channel edge image X^E. After concatenated X^E with X_{real} , it passed through the generator. Simultaneously, X^E undergoes the same downsampling process. The generator outputs X_f after extracting and merging semantic and structural features. The target image y and X_f will be put into the feature extraction network F. The Gram matrices of the feature maps are used to calculate the *Style Loss*. The discriminator is responsible for distinguishing between real and fake images.

3.2 Extraction of edge features

We evaluated EG-DUNet using both test and training data from the MITOS-ATYPIA ICPR'14. The dataset consisted of 1000 histopathology images with 16 standard Hematoxylin and Eosin stained (H&E stained) slides. These images were divided into 11 for training and 5 for testing. All aligned images are from the same slide, but two different slide scanners were used: the Aperio and the Hamamatsu.

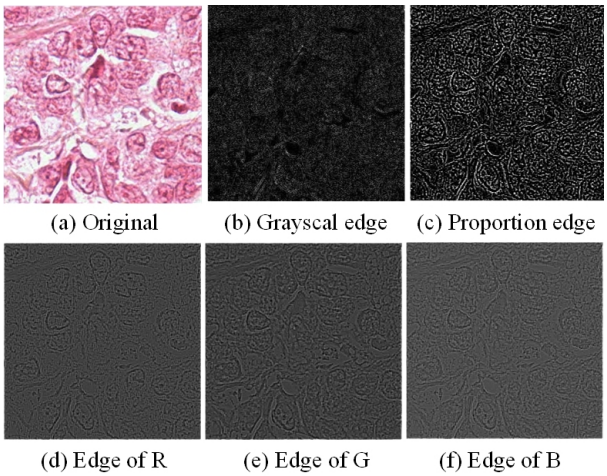

Fig. 3. Edge extraction with different channels and methods

H&E staining method is commonly employed in medical pathology images, distinguishing different structural components through color. The cell nucleus appears blue, the cytoplasm usually appears light red, and the extracellular collagen fibers appear red, facilitating the observation of microstructures. Edge features aid in locating the edges of the nucleus and cytoplasm in pathology section images, thereby enhancing the interpretability of the image and the accuracy of doctors' diagnoses, playing a crucial role in pathology section images. Therefore, because of the characteristics of H&E staining, the edge features in the RGB channels are distinct, as shown in (d)-(f) of Fig. 3.

Traditional edge extraction methods involve converting RGB images to grayscale and then applying different kernels, such as the Laplacian kernel, for computation. For medical stained images, the grayscale conversion method results in the loss of some edge structural features, as depicted in (b) of Fig. 3, leading to less pronounced edge features. In response to this, we analyzed the feature distribution in RGB channels and proposed conducting edge detection in each channel, followed by combining the RGB pixel distributions. Verified by experiment, the combination in a 4:4:2 ratio proves to be more effective in clearly extracting

edges. Additionally, we proposed a new-sized Laplacian convolution kernel to effectively preserve edge features, the result is shown in Fig. 3(c).

The generator of the model in this paper first extracts the edge features of the input slice image using Laplace kernel to obtain the edge features of a single channel of the input slice image. Highlight the details and edge information of pathology slice images and improve the perception of cell and tissue structures. Next, single-channel edge features are connected with RGB three-channel to obtain spliced data. The single-channel edge features are spliced with the three-channel raw image to further enhance the presentation of the data. This allows the generator to focus on both the color information and edge details of the original image. This combination helps to preserve the overall appearance and color of the image while highlighting the edge information. Stitching edge features with RGB images to obtain stitched data helps to improve the robustness of the generator.

3.3 Dual UNet structure for translating images

The current model structure used by generators in GAN is usually resnet. The residual blocks in its structure are mainly focused on the deep representation of features, and for the coloring normalization task, this structure may focus on more abstract features in general and ignore some local details. And for spliced data, which contains both RGB channel information of the original image and edge features. ResNet does not explicitly model multi-scale information, which lead to some limitations in the fusion of structural and semantic features.In medical imaging, the UNet model, due to its incorporation of both upsampling and downsampling processes, is capable of producing images with higher resolution.

In this paper, a dual UNet network is designed to learn the correlation between edge localization and overall image structure for edge features as well as spliced data. As shown in Fig. 2(b) , After inputting X^E and X_r, they undergo concurrent downsampling using 3×3 convolutional kernels, BN layers, ReLU activation functions, and pooling operations within two identical downsamplers. In the fifth layer, a 16×16 convolutional layer is achieved, followed by upsampling to reconstruct the image. Skip connections are employed at each downsampling layer for both X^E and X_r. The X_f is restored to a size of 256×256 pixels.

Additionally, the discriminator as shown in Fig. 2(a) , X_{real} and X_f are fed into a pre-trained deep convolutional classifier feature to obtain the feature maps, and the mean-square distance between these activations [16]. This distance is used in the subsequent perceptual loss function to help preserve subtle salient structural content when the input image is transformed to the output domain [17]. In the next subsections, we describe in detail all the loss functions used to train the network, based on which makes it possible for the method of ours to efficiently perform the task of sliced image normalization.

3.4 Loss Function

In the context of staining tasks, the commonly used loss function is L1 loss. However, it primarily focuses on the differences between pixel values, leading to color inconsistencies and biases, especially in edge staining. Therefore, we propose the utilization of multiple loss functions in combination to enhance overall performance.

The computation of the adversarial loss $Loss_{cheat}$ is based on the discriminator's estimate of the realism of the generated image. Binary cross-entropy loss not only focuses on the overall image distribution, but also on fine-grained feature matching, as it computes the difference between the generated and real images at the pixel level. In pathology, this helps to ensure that the generated images are not only similar overall, but also match the real image in terms of detail and structure.

$$\begin{aligned} Loss_{cheat} = -\tfrac{1}{K} \sum_{i=1}^{K} (y_{real} \cdot \log(\sigma(fake\_D\_logits_i)) \\ +(1 - y_{real}) \cdot \log(1 - \sigma(fake\_D\_logits_i))) \end{aligned} \tag{2}$$

K is the number of samples. The σ is a sigmoid function that maps logits to the range (0,1). $fake\_D\_logits_i$ is the logits of the ith sample generated by the generator. y_{real} is the label, which is usually 0 (for false) for images generated by the generator, so the $(1 - y_{real})$ part corresponds to the $log(1 - D(G(x)))$ of the image generated by the $log(1 - D(G(x)))$ of the image generated by the generator, where $D(G(x))$ is the output of the discriminator to the generated image.

The perceptual loss function $Loss_{AfB}$ helps to ensure that the generated image is similar to the target image in terms of specific details and structure, providing an effective loss metric for normalization of pathology slice images. The perceptual loss function is in essence a feature-based Mean Squared Error (MSE). The loss math is specified as follows: suppose we have two feature vectors representing the features $featfakeB$ of the generated image and the features $featrealB$ of the target image. The elements of these two feature vectors are f_{fakeB_i} and f_{realB_i}. The mean square error loss at the feature level is computed as:

$$Loss_{AfB} = \frac{1}{M} \sum_{i=1}^{M} (f_{realB_i} - f_{fakeB_i})^2 \tag{3}$$

Where M is the dimension of the feature vector, this loss calculates the squared difference between the features of the generated image and the features of the target image, averaged to obtain the overall loss.

The style loss is calculated using the Gram matrix, which is a correlation matrix between different channels in the feature map to capture the texture and style information of the image. Here is how the style loss calculation is represented in a mathematical formula. Suppose $featfakeB$ is the feature map

of the generated image and $featrealB$ is the feature map of the target image. The Gram matrix is calculated as follows:

$$G_{fakeB}(i,j) = \sum_{k} featfakeB(i,k) \cdot featfake(j,k) \tag{4}$$

For the feature map $featrealB$, the elements of its Gram matrix $G_{realB}(i,j)$ are computed as above. Style Loss $Loss_{style}$ can be used to measure the stylistic difference between the generated image and the target image by calculating the MSE between two Gram matrices:

$$Loss_{style} = \frac{1}{N^2} \sum_{i,j} \left(G_{fakeB}(i,j) - G_{realB}(i,j)\right)^2 \tag{5}$$

The final overall loss ($Loss$) is a linear combination of these above four components. Some of the weights are controlled by corresponding hyperparameters that can be tuned to the specific task and dataset.

$$Loss = Loss_{cheat} + \delta \cdot Loss_{L1} + \lambda \cdot Loss_{AfB} + Loss_{style} \tag{6}$$

δ, λ are the weight adjustment factors for $Loss_{L1}$ and $Loss_{AfB}$, respectively, which are used to adjust the contribution of $Loss_{L1}$ and $Loss_{AfB}$ to the overall loss. The final loss function combines feature-level similarity, pixel-level differences, adversarial, and stylistic consistency. For example, $Loss_{L1}$ helps to maintain the structural consistency of the image, while $Loss_{style}$ helps to ensure that the generated image is stylistically consistent with the target image, thus making the generated image more natural and close to the target. The use of adversarial loss helps the generator to learn a more realistic image, thus improving the realism of the generated image. This enables the model to integrate multiple aspects of image quality and consistency, providing a new solution to effectively address the problems of structure, fidelity and stylistic consistency in medical image normalization.

4 EXPERIMENTAL

4.1 Implementation Details

The experimental setup includes Ubuntu 18.04, NVIDIA GeForce GTX 2080Ti x1, Intel Core i7-4790k quad-core CPU running @ 4.00 GHz. The experiments are conducted using the deep learning framework of Python 3.6 and Pytorch 1.6.0.We employed the Adam optimizer with an initial learning rate of e-4. The number of training epochs was set to 100. All models were implemented using PyTorch.

4.2 Evaluation Metrics

In order to quantify the extent to which different methods preserve the salient structure of the original slice images, we used the Structural Similarity Index (SSIM) , Peak Signal to Noise Ratio (PSNR), Root Mean Square Error (RMSE), Mean Square Error (MSE) and Universal Quality Image Index (UQI). We also used Multi-Scale Structural Similarity (MS-SSIM) to enhance the flexibility of image evaluation[18] and Learned Perceptual Image Patch Similarity (LPIPS), a learning-based perceptual similarity metric that aligns better with human perception[19] . These metrics evaluate the generated results from multiple perspectives, such as brightness, contrast, signal-to-noise ratio, structural, pixel-level differences, human perception, etc., in order to fully validate the excellent performance of this paper's method[20].

4.3 Experimental Results

Ablation Experiments Conducting ablation experiments in the pathology slice image normalization task helps to understand the contribution of generator architecture, loss function to performance. The ablation experiments results in Table 1 provide insight into the performance of different components and design choices for normalizing pathology slice images.

Table 1. The evaluation metric values of the ablation experimental results.

Metrics	UNet	UNet +loss	Dual-UNet	**Ours**
SSIM↑	0.7264	**0.7687**	0.7558	**0.7783**
PSNR↑	23.3793	**24.5169**	23.8259	**24.6224**
MS-SSIM↑	0.8989	**0.9145**	0.9101	**0.9174**
RMSE↓	0.0702	**0.0625**	0.0677	**0.0627**
MSE↓	0.0053	**0.0044**	0.0051	**0.0045**
LPIPS↓	0.1301	0.1365	**0.1175**	**0.1269**
UQI↑	0.9875	**0.9896**	0.9881	**0.9892**

As a benchmark combination, Unet exhibits relatively low values in evaluation metrics such as SSIM, PSNR, MS-SSIM, and RMSE. This suggests certain limitations in image quality and structure preservation when using a generator based solely on the Unet network. In the absence of a designed loss function, dual UNet shows a marginal improvement across all metrics compared to Unet, indicating that the introduction of the dual UNet model with edge extraction contributes to enhanced performance. Upon the introduction of the designed loss function, UNet+loss significantly improves across most of metrics, particularly in SSIM, PSNR, MS-SSIM, RMSE, and MSE. This validates the effectiveness of the designed loss function in enhancing both image quality and structure

preservation.Continuing with the dual UNet model that incorporates the edge extraction module and using the style loss function further, EG-DUNet achieves optimal performance in terms of SSIM, PSNR, and MS-SSIM, while exhibiting suboptimal performance in RMSE, MSE, LPIPS, and UQI, with only minimal differences from the optimal values. This further emphasizes the synergistic effect between the edge extraction strategy and the designed loss function, providing the model with improved overall performance. In conclusion, by gradually introducing the edge extraction strategy and the designed loss function, our proposed method, EG-DUNet , attains the best performance in the task of pathology slice image normalization. These experimental results once again demonstrate the effectiveness of our approach in maintaining both the structural and stylistic aspects of slice images during the normalization task, providing crucial insights into the contributions of individual components to the overall performance.

Table 2. The evaluation metric values of the compared experimental results.

Metrics	Traditional Methods			Deep Learning Methods			**Ours**
	Reinhard	Macenko	Vahadane	StainGAN	StainNet	MultiPathGAN	
SSIM↑	0.62952	0.66371	0.67802	0.70209	0.69090	**0.73796**	**0.77834**
PSNR↑	19.95075	21.70460	21.17302	22.39701	22.50131	**23.00714**	**24.62241**
MS-SSIM↑	0.47529	0.50146	0.52039	0.88334	0.88034	**0.88421**	**0.91741**
RMSE↓	0.30928	0.27850	0.26849	0.12363	0.11856	**0.08018**	**0.06269**
MSE↓	0.09574	0.07724	0.07174	0.01528	0.01415	**0.00903**	**0.00454**
LPIPS↓	0.56773	0.54584	0.54028	0.24411	0.20419	**0.17802**	**0.12692**
UQI↑	0.73569	0.75802	0.76031	0.97350	0.93538	**0.97823**	**0.98921**

Experiments comparing to existing methods In this study, we provide a comprehensive comparison of the proposed EG-DUNet methods, drawing on three traditional methods Reinhard, Macenko,and Vahadane and three deep learning-based methods StainGAN, StainNet, and MultiPathGAN as controls. This extensive comparison framework aims to provide insight into the performance of EG-DUNet relative to methods from different paradigms in the task of sliced image normalization. Meanwhile, a series of evaluation metrics in Section 4.2 are used to comprehensively measure the effectiveness of the methods. Table 2 shows the performance of each method on different metrics in detail.

4.4 Visualization of Experiment

Fig. 4 shows the original and the target image on the leftmost side, and the others are the six methods and the experimental results of our method. the Reinhard method is consistent with the target image in terms of color tone, but its contrast is low. the Vahadan and Macenko method results are more consistent

with the target image in terms of structure, but the overall style is more different from the target image. The results of the three deep learning-based methods are basically consistent with the target image in structure, but there is a large gap between them and the target image in details such as the edges, and they are also far from each other in the overall style. The image generated by our proposed method is not only consistent with the target image in the localization of the edges, structure, and details, but also highly uniform with the target image in the overall contrast, color, and style.

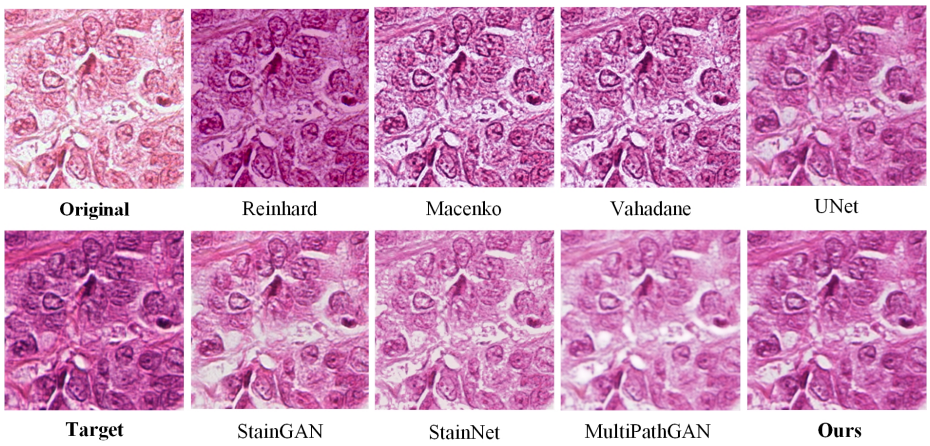

Fig. 4. Visualization comparison of staining result of different algorithms on the MITOS-ATYPIA ICPR'14 sample

5 CONCLUSION

In this paper, we propose the EG-DUNet model, which enhances color consistency and edge features in staining by using a dual Unet network with a custom edge extraction module and the incorporation of style loss through GAN. To address significant variations in image color caused by differences in laboratory reagents and scanning devices, we add style loss to mitigate color distortions. Additionally, we design a novel channel-wise proportional edge extraction module to address the issue of unclear edges in stained images. Our network demonstrates superior performance compared to other models on the publicly available MITOS-ATYPIA ICPR'14 dataset.

References

1. Melo, R.C.N., Raas, M.W.D., Palazzi, C., Neves, V.H., Malta, K.K., Silva, T.P.: Whole slide imaging and its applications to histopathological studies of liver disor-

ders. In: Frontiers in medicine, pp. 310. (2020)
2. Reddy, B.S., Sathish, A.: A hybrid method for magnetic resonance brain images classification and segmentation using soft computing techniques. Artificial Intelligence and Technology **3**(3), 134–141 (2023)
3. Mani, R.K.C., Kamalakannan, J., Rangaiah, Y.P., Anand, S.: A bio-inspired method for breast histopathology image classification using transfer learning. Artificial Intelligence and Technology **2**(5), 99–110 (2016)
4. Jose, L., Liu, S., Russo, C., Nadort, A., Ieva, A.D.: Generative adversarial networks in digital pathology and histopathological image processing: A review. Pathology Informatics **12**(1), 43 (2021)
5. Bianconi, F., Kather, J.N., Reyes-Aldasoro, C.C.: Experimental assessment of color deconvolution and color normalization for automated classification of histology images stained with hematoxylin and eosin. Cancers **12**(11), 3337 (2020)
6. Bejnordi, B.E., Timofeeva, N., Otte-Holler, I., Karssemeijer, N., Laak, A.W.M.: Quantitative analysis of stain variability in histology slides and an algorithm for standardization. In: 9th Medical Imaging 2014: Digital Pathology, pp. 45–51. SPIE, Location (2014)
7. Tellez, D., Litjens, G., Bandi, P., Bulten, W., Bokhorst, J., Ciompi, F., Laak, J.V.D.: Quantifying the effects of data augmentation and stain color normalization in convolutional neural networks for computational pathology. Medical image analysis **58**, 101544 (2019)
8. Dimitriou, N., Arandjelovic, O.: Magnifying Networks for Images with Billions of Pixels. ArXiv abs/2112.06121 (2021) https://api.semanticscholar.org/CorpusID:245124534
9. Reinhar, E., Adhikhmin, M., Gooch, B., Shirley, P.: Color transfer between images. International Proceedings on Proceedings **21**(5), pp. 34–41. Publisher, Location (2001)
10. Aswathy, M.A., Jagannath, M.: Dual stage normalization approach towards classification of breast cancer. IETE Journal of Research **68**(4), 3074–3085 (2022)
11. Salvi, M., Michielli, N., Molinari, F.: Stain color adaptive normalization (SCAN) algorithm: Separation and standardization of histological stains in digital pathology. Computer methods and programs in biomedicine **193**, 105506 (2020)
12. Macenko, M., Niethammer, M., Marron, J.S., Borland, D., Woosley, J.T., Guan, X., Schmitt, C., Thomas, N.E.: A method for normalizing histology slides for quantitative analysis. In: 2009 IEEE international symposium on biomedical imaging: from nano to macro, pp. 1107–1110. IEEE (2009)
13. Vahadane, A., Peng, T., Sethi, A., Albarqouni, S., Wang, L., Baust, M., Steiger, K., Schlitter, A.M., Esposito, I., Navab, N.: Structure-preserving color normalization and sparse stain separation for histological images. IEEE transactions on medical imaging **35**(8), 1962–1971 (2016)
14. Zhu, J., Park, T., Isola, P., Efros, A.A.: Unpaired image-to-image translation using cycle-consistent adversarial network. In: Proceedings of the IEEE international conference on computer vision, pp. 2223–2232. IEEE (2017)
15. Nazki, H., Arandjelovic, O., Um, I.H., Harrison, D.: Multipathgan: Structure preserving stain normalization using unsupervised multi-domain adversarial network with perception loss. In: Proceedings of the 38th ACM/SIGAPP Symposium on Applied Computing, pp. 1197–1204. (2023)
16. Ledig, C., Theis, L., Huszar, F., Caballero, J., Cunningham, A., Acosta, A., Aitken, A., Tejani, A., Totz, J., Wang, Z.: Photo-realistic single image super-resolution using a generative adversarial network. In: Proceedings of the IEEE conference on computer vision and pattern recognition, pp. 4681–4690. (2017)

17. Nazki, H., Yoon, S., Fuentes, A., Park, D.S.: Unsupervised image translation using adversarial networks for improved plant disease recognition. Computers and Electronics in Agriculture **168**, 105117 (2020)
18. Simoncelli, E.P., Wang, Z., Bovik, A.C.: Multiscale structural similarity for image quality assessment. In: The Thirty-Seventh Asilomar Conference on Signals, Systems, and Computers, pp. 1398–1402. (2003)
19. Isola, P., Zhang, R., Efros, A.A.: The unreasonable effectiveness of deep features as a perceptual metric. In: Proceedings of the IEEE conference on computer vision and pattern recognition, pp. 586–595. IEEE (2018)
20. Shen, Y., Luo, Y., Shen, D., Ke, J.: Randstainna: Learning stain-agnostic features from histology slides by bridging stain augmentation and normalization. In: International Conference on Medical Image Computing and Computer-Assisted Intervention, pp. 212–221. Springer (2022)